Molecular Human Reproduction, Vol.17, No.8 pp. 500–510, 2011
Advanced Access publication on May 23, 2011 doi:10.1093/molehr/gar040

MHR Basic science of reproductive medicine

NEW RESEARCH HORIZON ***Review***

Mathematical modeling of calcium signaling during sperm hyperactivation

S.D. Olson [1], L.J. Fauci [1], and S.S. Suarez [2,*]

[1]Department of Mathematics, Tulane University, New Orleans, LA 70115 USA [2]Department of Biomedical Sciences, Cornell University College of Veterinary Medicine, T5-002B Veterinary Research Tower, Ithaca, NY 14853 USA

*Correspondence address. Tel: +1-607-253-3589; Fax: +1-607-253-3541; E-mail: sss7@cornell.edu

Submitted on November 29, 2010; resubmitted on January 17, 2011; accepted on May 17, 2011

ABSTRACT: Mammalian sperm must hyperactivate in order to fertilize oocytes. Hyperactivation is characterized by highly asymmetrical flagellar bending. It serves to move sperm out of the oviductal reservoir and to penetrate viscoelastic fluids, such as the cumulus matrix. It is absolutely required for sperm penetration of the oocyte zona pellucida. In order for sperm to hyperactivate, cytoplasmic Ca^{2+} levels in the flagellum must increase. The major mechanism for providing Ca^{2+} to the flagellum, at least in mice, are CatSper channels in the plasma membrane of the principal piece of the flagellum, because sperm from CatSper null males are unable to hyperactivate. There is some evidence for the existence of other types of Ca^{2+} channels in sperm, but their roles in hyperactivation have not been clearly established. Another Ca^{2+} source for hyperactivation is the store in the redundant nuclear envelope of sperm. To stabilize levels of cytoplasmic Ca^{2+}, sperm contain Ca^{2+} ATPase and exchangers. The interactions between channels, Ca^{2+} ATPases, and exchangers are poorly understood; however, mathematical modeling can help to elucidate how they work together to produce the patterns of changes in Ca^{2+} levels that have been observed in sperm. Mathematical models can reveal interesting and unexpected relationships, suggesting experiments to be performed in the laboratory. Mathematical analysis of Ca^{2+} dynamics has been used to develop a model for Ca^{2+} clearance and for CatSper-mediated Ca^{2+} dynamics. Models may also be used to understand how Ca^{2+} patterns produce flagellar bending patterns of sperm in fluids of low and high viscosity and elasticity.

Key words: spermatozoa / sperm motility / mathematical model / CatSper / Ca^{2+} signaling

Introduction: definition of hyperactivation

Hyperactivation is a type of motility that is characterized by a highly asymmetrical and high-amplitude flagellar beat pattern (Yanagimachi, 1994; Ishijima *et al.*, 2006) which gives rise to a whip-like movement of the flagellum that can produce circular, figure eight or zigzag swimming trajectories. Initiation and maintenance of hyperactivated motility is associated with an increase in Ca^{2+} concentration in the flagellum (Suarez *et al.*, 1993; Ho and Suarez, 2001b; Ho *et al.*, 2002; Carlson *et al.*, 2005). Hyperactivation can be induced in sperm with the use of Ca^{2+} ionophores A23187 or ionomycin, which facilitate Ca^{2+} transport across the plasma membrane (Suarez *et al.*, 1987, 1992; Marquez and Suarez, 2007; Xia *et al.*, 2007). Pharmacological agents such as caffeine (Ho and Suarez, 2001b), procaine (Marquez and Suarez, 2004), thimerosal (Ho and Suarez, 2001b; Marquez *et al.*, 2007) and thapsigargin (Ho and Suarez, 2001b, 2003) have all been shown to induce asymmetrical beating resembling physiological hyperactivation by increasing intracellular Ca^{2+}, by allowing increased Ca^{2+} transport across membranes, or by causing release of Ca^{2+} from stores. Sperm that have been demembranated by detergent and reactivated by adding exogenous ATP in a special 'intracellular' medium, display the symmetrical beat pattern characteristic of activated motility in ~50 nM Ca^{2+}, but switch to asymmetrical beating characteristic of hyperactivation when Ca^{2+} is increased to about 400 nM (Ho *et al.*, 2002). Therefore, it is believed that Ca^{2+} is the primary second messenger that triggers hyperactivated motility.

In this review, we first discuss the movement of sperm through the female reproductive tract in order to introduce the roles played by hyperactivation in bringing about fertilization. Next, we review mechanisms of modulating Ca^{2+} levels in sperm and the molecular targets of Ca^{2+}. Finally, we will describe how mathematical modeling can help us to understand how Ca^{2+} distributes in sperm to trigger and support hyperactivation.

Hyperactivation in the context of movement of sperm through the mammalian female reproductive tract

The propulsion of sperm via flagellar bending is vital for the sperm to move through the female reproductive tract. When sperm are moved out of the epididymis during ejaculation and come into contact with

secretions of the male accessory glands, soluble adenylyl cyclase (SACY) is activated and raises the intracellular level of cAMP (Chen *et al.*, 2000; Carlson *et al.*, 2007). This stimulates a cascade of protein phosphorylation to activate sperm motility (Tash and Means, 1982, 1983; San Agustin and Witman, 1994). Activated motility is characterized by symmetrical and low-amplitude flagellar beating that produces linear swimming trajectories (reviewed by Turner, 2003).

In humans, sperm are inseminated into the anterior vagina and quickly enter the cervix. There is evidence that sperm pass through the cervix by entering mucus filled microchannels in the periphery of the cervical canal, which lead them to the uterine cavity (Mattner, 1968; Mullins and Saacke, 1989; Suarez, 2010).

The uterus produces coordinated waves of myometrial smooth muscle contractions during the late follicular phase in humans and estrus in non-primates, which may serve to wash sperm toward the uterotubal junction (reviewed in Suarez and Pacey, 2006).

In order to pass through the uterotubal junction into the oviduct, sperm must not only possess normal motility (Smith *et al.*, 1988; Shalgi *et al.*, 1992), but also specific surface proteins on their heads (Yanamaguchi *et al.*, 2009). The role of these proteins in enabling sperm to swim through the junction is not understood, although it has been proposed that the proteins serve to adhere sperm lightly to the epithelial lining of the junction, to enable them to move against a gentle fluid outflow from the oviduct (Suarez, 2010).

Most sperm that enter the oviduct soon bind to the mucosal epithelium, which serves to hold them in a storage reservoir (DeMott and Suarez, 1992; Suarez and Pacey, 2006). Binding involves specific interactions between proteins on sperm and receptors on the oviductal epithelium. The interaction of sperm with the oviductal epithelium serves to maintain their ability to fertilize while they are in storage (Pollard *et al.*, 1991; Kervancioglu *et al.*, 1994; Lloyd *et al.*, 2008).

As the time of ovulation approaches, sperm are gradually released from the reservoir. There is evidence that release is brought about by loss of the oviduct-binding proteins (Gwathmey *et al.*, 2003, 2006; Ignotz *et al.*, 2007), as well as hyperactivation of sperm motility (DeMott and Suarez, 1992; Ho *et al.*, 2009). It is likely that the gradual loss of the binding proteins reduces the binding strength, enabling the deep flagellar bends produced by hyperactivated sperm to tear sperm off of the epithelium. Both hyperactivation and shedding of binding proteins have been associated with sperm capacitation, which is defined as a series of physiological and molecular changes that impart on the sperm the ability to fertilize the oocyte (Visconti, 2009).

When sperm move beyond the oviductal reservoir, they continue to use hyperactivated motility. Within the oviduct, hyperactivated motility is observed in sperm near the site of fertilization (Katz and Yanagimachi, 1980; Suarez and Osman, 1987). Hyperactivation has been shown to enable sperm to swim effectively through highly viscoelastic fluid, such as oviductal mucus and the matrix of the cumulus oophorus (Suarez *et al.*, 1991; Suarez and Dai, 1992). When sperm finally reach the oocyte within the cumulus oophorus, they require hyperactivation in order to penetrate its zona pellucida (Stauss *et al.*, 1995; Quill *et al.*, 2001; Ren *et al.*, 2001).

As the sperm nears the oocyte, chemical cues from the latter and/or its surroundings may modify the flagellar beat pattern in order to guide the sperm to the oocyte via a process of chemotaxis (Eisenbach, 2007; Chang and Suarez, 2010). The relationship of chemotaxis to hyperactivation is not well understood, but since sperm begin to hyperactivate in the lower oviduct, far from the site of fertilization, it has been proposed that chemotactic factors modulate the flagellar beat of hyperactivated sperm to re-direct them toward the oocyte (Chang and Suarez, 2010). There is evidence that Ca^{2+} signaling plays a role in the chemotactic response (Spehr *et al.*, 2003, 2004) in addition to its role in triggering hyperactivation. Progesterone has been implicated as a chemoattractant for human sperm (Teves *et al.*, 2006), although, at micromolar levels, it can also induce acrosome reactions (Osman *et al.*, 1989; Baldi *et al.*, 1998; Bedu-Addo *et al.*, 2007).

Much remains to be learned about regulation of sperm flagellar beat patterns and their role in promoting the movement of sperm through the female reproductive tract and to the oocyte. Nevertheless, it is clear that Ca^{2+} signaling plays a vital role in the regulatory processes.

Ca^{2+} signaling modulates sperm motility

The flagellar bend amplitude and the asymmetry of the flagellar beat of mammalian sperm waveforms have been found to be highly dependent on the intracellular Ca^{2+} concentration, and thus Ca^{2+} plays a key role in hyperactivating sperm. The Ca^{2+} that triggers hyperactivation *in vivo* may originate from the opening of Ca^{2+} channels in the plasma membrane or release of Ca^{2+} from intracellular stores, or both, acting together (Jimenez-Gonzalez *et al.*, 2006; Suarez, 2008). Cytoplasmic Ca^{2+} levels also depend on Ca^{2+} clearance mechanisms that transfer Ca^{2+} out of the cell or into mitochondria or Ca^{2+} storage organelles. The next few sections will deal with the mechanisms of increasing cytoplasmic Ca^{2+} levels in order to trigger and maintain hyperactivated motility.

Plasma membrane Ca^{2+} channels

CatSper channels, located on the plasma membrane of the principal piece (Fig. 1; Ren *et al.*, 2001; Quill *et al.*, 2003; Xia *et al.*, 2007), are the primary source of Ca^{2+} flux into the cytosol for hyperactivation (Kirichok *et al.*, 2006). CatSper channels are pH and voltage dependent Ca^{2+} permeable ion channels that are absolutely required for hyperactivated motility and are only found on sperm (Ren *et al.*, 2001; Quill *et al.*, 2003; Carlson *et al.*, 2003, 2005; Qi *et al.*, 2007; Xia *et al.*, 2007). CatSper channels are necessary for sperm to ascend beyond the oviductal reservoir (Ho *et al.*, 2009) and are required for sperm penetration of the zona pellucida of the oocyte (Ren *et al.*, 2001; Quill *et al.*, 2003). The CatSper proteins that form the ion channel contain six transmembrane segments, with a voltage-sensor S4 domain and a pore region that is Ca^{2+} selective (Ren *et al.*, 2001; Qi *et al.*, 2007). Four CatSper proteins have been identified: CatSper-1 (Ren *et al.*, 2001), -2 (Quill *et al.*, 2003), -3 and -4 (Lobley *et al.*, 2003; Jin *et al.*, 2007) that together form the subunits of the Ca^{2+} channel. In addition to the subunits that directly form the channel, other subunits associate with the channel complex, such as CatSperβ (Liu *et al.*, 2007) and CatSperγ (Wang *et al.*, 2009), and are thought to regulate channel activity.

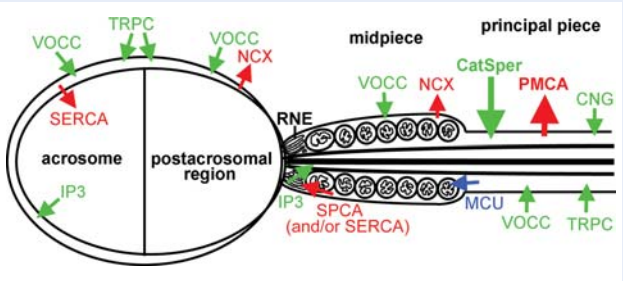

Figure 1 Ca^{2+} channels and pumps that have been immunolocalized in mammalian sperm. Arrows indicate the most common direction of Ca^{2+} movement caused by these entities in most cell types. The chief channels and pumps involved in hyperactivation are CatSper channels and PMCA, which are indicated by large arrows. Others that have been identified include the following: sarcoplasmic/endoplasmic reticular Ca^{2+} ATPase (SERCA), IP_3-gated channels (IP3); voltage-operated Ca^{2+}channels (VOCC), TRPC Ca^{2+} channels, secretory pathway Ca^{2+} ATPase (SPCA), NCX, mitochondrial uniporter (MCU) and CNG Ca^{2+} channels.

Sperm from CatSper null mice cannot hyperactivate and suffer a general decline in motility over time (Qi *et al.*, 2007; Quill *et al.*, 2003). Even the initial motility of CatSper null sperm is abnormal, which may be the result of abnormally low resting levels of Ca^{2+} (Marquez *et al.*, 2007). The flagellar bend amplitudes of CatSper null sperm are low, but can be raised to normal prehyperactivated levels with the application of thimerosal, which triggers release of Ca^{2+} from stores (Marquez *et al.*, 2007). Also, reducing Ca^{2+} levels in wild type sperm by loading sperm with the cell-permeant Ca^{2+} chelator BAPTA-AM produces abnormal motility resembling that of CatSper null sperm. Therefore CatSper channels may be involved in providing sufficient Ca^{2+} for activated, as well as hyperactivated, motility (Marquez *et al.*, 2007).

A pH-sensitive efflux of K^+ has been identified and is thought to aid in the hyperpolarization of the membrane, which would maximize Ca^{2+} entry through CatSper channels. The channel responsible for the K^+ efflux has been identified as KSper, a sperm-specific channel, which co-localizes with CatSpers in the principal piece of the sperm flagellum (Navarro *et al.*, 2007).

In addition to CatSper channels, a variety of Ca^{2+} channels have been identified in mammalian sperm, mostly by channel-specific antibodies. Various voltage-operated Ca^{2+} channels (VOCCs) have been detected in mouse and human sperm (Fig. 1; Wiesner *et al.*, 1998; Westenbroek and Babcock, 1999; Wennemuth *et al.*, 2000; Ren *et al.*, 2001; Sakata *et al.*, 2002; Quill *et al.*, 2003; Trevino *et al.*, 2004; Carlson *et al.*, 2005). The VOCCs are a family of transmembrane, channel-forming proteins that are composed of an $\alpha 1$ (pore-forming) subunit and several other auxiliary subunits (Catterall, 2000; Ertel *et al.*, 2000; Jimenez-Gonzalez *et al.*, 2006). Through immunostaining and pharmacological analyses, low-voltage activated (T-type) and high-voltage activated (L-, R-, P/Q and N-type) VOCCs have been identified in sperm (Arnoult *et al.*, 1996; Benoff, 1998; Wennemuth *et al.*, 2000; Felix, 2005).

Capacitative Ca^{2+} entry via transient receptor potential channels (TRPC) may influence sperm motility and play a role in resequestration of Ca^{2+} into stores. TRPC channels are made of six transmembrane units and studies have identified four types in sperm, TRPC-1, 3, 4 and 6 (Trevino *et al.*, 2001; Castellano *et al.*, 2003). TRPC channels have been localized to the principal piece of human sperm flagellum and the head (Fig. 1; Castellano *et al.*, 2003; Jimenez-Gonzalez *et al.*, 2006).

Cyclic nucleotide-gated (CNG) Ca^{2+} channels have been identified on the flagella of bull sperm using antibodies (Fig. 1; Wiesner *et al.*, 1998). When bull or mouse sperm were treated with cGMP or cAMP via cell-permeant analogs, intracellular Ca^{2+} increased (Wiesner *et al.*, 1998; Xia *et al.*, 2007); however, the role played by CNG Ca^{2+} channels in hyperactivation is difficult to determine, because mouse sperm that lack CatSper channels do not respond to cyclic nucleotides. These channels may not be required for hyperactivation, or they may interact somehow with CatSper channels.

Ca^{2+} stores and their relevant pumps and receptors

The redundant nuclear envelope (RNE), which is located at the base of the flagellum (Fig. 1) contains a Ca^{2+} store (Ho and Suarez, 2001b, 2003). This store is likely to be an inositol 1,4,5-trisphosphate (IP_3)-gated store, because the IP_3 receptor has been localized by antibodies to a portion of the RNE in bull sperm, as well calreticulin, which is the Ca^{2+}-binding protein in reticular stores (Ho and Suarez, 2001b, 2003). Thapsigargin, a Ca^{2+} ATPase inhibitor that depletes intracellular Ca^{2+} stores, induces an increase in intracellular Ca^{2+} great enough to switch on hyperactivation, even in the absence of available external Ca^{2+} (Ho and Suarez, 2003). The increase in intracellular Ca^{2+} that occurs during hyperactivation has been proposed to derive from both the opening of CatSper plasma membrane channels and the release of Ca^{2+} from the RNE store via IP_3-gated channels (Ho and Suarez, 2001b, 2003). At this time, however, it is not known whether Ca^{2+} release from the RNE normally plays a role in hyperactivation or if it only serves to modulate hyperactivated motility. Recent observations indicate that release from the store actually produces a reversed pattern of hyperactivation (Marquez *et al.*, 2007; Chang and Suarez, 2010, 2011). In mouse sperm, the direction of the dominant, high-amplitude bend of flagellum can be determined, because the hook of the head of mouse sperm can serve as a reference point. The dominant flagellar bend of mouse sperm hyperactivated during capacitation, or by pharmacological activation of CatSper channels using procaine or 4-aminopyridine, was primarily oriented in the same direction as the hook of the sperm head. In contrast, the dominant bend in sperm hyperactivated by thimerosal, which triggers release of Ca^{2+} from internal stores, was oriented in the opposite direction of the hook in the head (see videos published in Chang and Suarez, 2011 http://www.biolreprod.org/content/early/2011/03/08/biolreprod.110.089789/suppl/DC1 with permission). It was proposed that release of Ca^{2+} from the RNE store serves to correct the course of hyperactivated sperm to re-orient sperm toward the oocyte and thus it may act as a mechanism of chemotaxis (Chang and Suarez, 2011). This phenomenon requires further investigation.

The acrosome also acts as an IP_3-gated Ca^{2+} store in sperm, which is thought to contribute to raising cytoplasmic Ca^{2+} to support the acrosome reaction (Walensky and Snyder, 1995; Herrick *et al.*,

2005; Lawson *et al.*, 2007). Sperm of CatSper-1 null mice can undergo the acrosome reaction even though they do not hyperactivate under capacitating conditions (Ren *et al.*, 2001; Quill *et al.*, 2003; Xia *et al.*, 2007). Stimulation of the IP_3 receptor with thimerosal can trigger hyperactivation (Ho and Suarez, 2001a), or the acrosome reaction (Herrick *et al.*, 2005), depending upon experimental conditions.

The sarcoplasmic endoplasmic reticulum Ca^{2+} ATPase (SERCA), which pumps Ca^{2+} from the cytoplasm into intracellular stores, has been immunolocalized to the midpiece and acrosomal region of human sperm (Lawson *et al.*, 2007). In other cell types, SERCA activity is highly sensitive to the inhibitor thapsigargin (Thastrup *et al.*, 1990). Inhibition generally produces a rise in cytoplasmic Ca^{2+} by releasing it from endoplasmic stores. Thapsigargin has been shown to stimulate hyperactivation in bull sperm (Ho and Suarez, 2001a, b) and the acrosome reaction in human sperm (Meizel and Turner, 1993; O'Toole *et al.*, 2000); however, the doses required to produce the effects are much higher than those required for other cell types (Harper *et al.*, 2005), indicating that the response may be non-specific or that the drug has poor penetration into the intracellular stores of sperm.

The secretory pathway Ca^{2+} ATPase (SPCA) could serve to refill sperm intracellular stores instead of, or along with, SERCA. SPCA has been immunolocalized to the posterior head or neck and the midpiece of human sperm (Fig. 1), where it could affect RNE stores (Harper *et al.*, 2005; Bedu-Addo *et al.*, 2008; Costello *et al.*, 2009). The SPCA pump in other cell types has been observed to transport Ca^{2+} with an affinity similar to that of SERCA pumps (Wuytack *et al.*, 2002).

Ca^{2+} clearance mechanisms

Sperm utilize Ca^{2+} clearance mechanisms to control intracellular Ca^{2+} levels (Wennemuth *et al.*, 2003; reviewed in Jimenez-Gonzalez *et al.*, 2006). Even though there exists a constant leak of Ca^{2+} from the extracellular fluid (which contain mM levels of Ca^{2+}) through the plasma membrane into the cytosol, activated sperm are still able to maintain a resting level of Ca^{2+} that ranges from about 40 nM in hamster and bull sperm (Suarez *et al.*, 1993; Ho *et al.*, 2002) to 100–250 nM in mouse sperm (Wennemuth *et al.*, 2003). The different levels reported may be due to species or experimental differences. For example, the measurements of Ca^{2+} levels in hamster and bull sperm were recorded at the specific body temperature of each species, whereas those of mouse sperm were performed at room temperature. In comparison with other cells types, the resting levels of astrocytes were reported to be 87 nM (Parpura and Haydon, 2000), while those of cultured skeletal myotubes were reported to be 116 ± 7 nM (Eltit *et al.*, 2010).

The primary mechanism of Ca^{2+} clearance in sperm, at least in the mouse, is via the plasma membrane Ca^{2+} ATPase (PMCA). The PMCA pumps use ATP to export a cytoplasmic Ca^{2+} ion out in exchange for one or two extracellular protons brought into the cytosol. Antibody labeling of PMCA shows a patchy distribution along the principal piece of the mouse sperm tail that tapers off distally toward the tip, similar to the distribution of CatSper channel subunits (Fig. 1; Wennemuth *et al.*, 2003; Okunade *et al.*, 2004). In addition, some faint antibody labeling has been detected on the midpiece and head (Okunade *et al.*, 2004). When the PMCA activity was depressed by raising the pH of the medium, other mechanisms cleared sperm cytoplasmic Ca^{2+}, but only to an intermediate level (Wennemuth *et al.*, 2003). The major isoform of PMCA expressed in mouse sperm is PMCA-4. PMCA-4 null mouse sperm quickly developed severely impaired motility when incubated under capacitating conditions that eventually produced hyperactivation in wild type sperm (Okunade *et al.*, 2004; Schuh *et al.*, 2004).

The Na^+/Ca^{2+} exchanger (NCX) is another mechanism of Ca^{2+} clearance in sperm, which can remove Ca^{2+} out of the cell or into an intracellular store. The NCX has been localized to the post-acrosomal region and flagellar midpiece in human sperm (Jimenez-Gonzalez *et al.*, 2006; Krasznai *et al.*, 2006), which differs from the distribution of PMCA-4 in mouse sperm (Fig. 1). When the intracellular Ca^{2+} concentration is high, the exchanger will export a Ca^{2+} ion out of the cytosol in exchange for the influx of three Na^+ ions. The NCX can reverse direction when sperm membranes are depolarized or when Na^+ is removed from the medium (Wennemuth *et al.*, 2003). The exchanger has been estimated to operate at about one-third the rate of PMCA in mouse sperm (Wennemuth *et al.*, 2003).

Mitochondria can act as Ca^{2+} buffers and remove Ca^{2+} from the cytosol (Nicholls and Chalmers, 2004). In other cell types, the mitochondrial Ca^{2+} uniporter (MCU) brings Ca^{2+} into energized mitochondria when intracellular Ca^{2+} is above 500 nM (Gunter *et al.*, 2000), as it may do in hyperactivated sperm. The mitochondria at the base of the flagellum lie very close to the RNE Ca^{2+} store and, in bull sperm, electron micrographs revealed that these mitochondria are uncoiled from the tightly wound mitochondrial helix in the flagellar midpiece, such that they associate closely with the RNE (Ho and Suarez, 2001a, b). Such a close association between the two types of organelles strongly suggests that they interact. On the other hand, treatment of bull sperm with CGP-37157 to inhibit the NCX did not prevent procaine induction of hyperactivation (Ho and Suarez, 2003). Also, in human sperm, application of the mitochondrial uncoupler 2,4-dinitrophenol had no effect on progesterone induction of Ca^{2+} oscillations (Harper *et al.*, 2004). It was found that treatment with protonophore carbonyl cyanide *m*-chlorophenyl hydrazone (CCCP) to depolarize the inner mitochondrial membrane and prevent Ca^{2+} uptake by the MCU has only a minor effect on Ca^{2+} clearance in mouse sperm (Wennemuth *et al.*, 2003). Thus, there is little evidence for a specific role of mitochondria in regulating Ca^{2+} levels in sperm flagella.

Where and how is Ca^{2+} acting to modify the waveform?

The exact mechanism and signaling pathway by which Ca^{2+} acts to trigger hyperactivated motility, transitioning from symmetrical to asymmetrical flagellar beating, is not known. In the flagellar axoneme, the hydrolysis of ATP on the dynein arms can be converted into force, which causes the microtubules to slide past one another. Sliding is converted to bending by the restraining influence of other structures in the axoneme (Lindemann and Lesich, 2010). The demembranated sperm model has helped us to understand where Ca^{2+} is acting to modify the waveform. When reactivated, bull sperm show symmetrical flagellar beating at ~50 nM Ca^{2+} and asymmetrical, hyperactivated beating at about 400 nM Ca^{2+} (Ho *et al.*, 2002). Similar results have

been seen in sea urchin sperm (Brokaw, 1979) and in rat sperm (Lindemann and Goltz, 1988). These observations indicate that the Ca^{2+} is acting directly at the axoneme, rather than at the plasma membrane or other cellular compartments. Further, in reactivated demembranated sea urchin sperm, it was demonstrated that Ca^{2+} regulates the activity of a specific group of dynein arms (Bannai *et al.*, 2000). Ni^{2+} and Cd^{2+} have been shown to block a specific subset of dyneins, presumably by binding to Ca^{2+} receptors (Kanous *et al.*, 1993; Lindemann *et al.*, 1995) and thereby indicating that there are receptors with different binding specificities for divalent cations.

Ca^{2+} can modify flagellar bending in several different ways. Mechanical effects such as changing the spoke length, nexin length or elasticity of the nexins could be induced by Ca^{2+} to modify the waveform (Lindemann and Kanous, 1995). One immediate target for Ca^{2+} is calmodulin (CaM) (Means *et al.*, 1982; Weinmann *et al.*, 1986; Bendahmane *et al.*, 2001), which has been localized to the principal piece of the flagellum (Schlingmann *et al.*, 2007). When CaM was extracted from demembranated bull sperm, motility could not be reactivated unless exogenous CaM was added back (Ignotz and Suarez, 2005).

Binding of Ca^{2+} to CaM could activate Ca^{2+}/CaM-dependent kinases (Marin-Briggiler *et al.*, 2005), which could phosphorylate an axonemal protein, resulting in a modification of the waveform (Suarez, 2008). CaM kinases have been identified in the flagella of bovine (Ignotz and Suarez, 2005) and human (Marin-Briggiler *et al.*, 2005) sperm. Peptide inhibitors of CaMKII, as well as a membrane-permeant inhibitor of CaMKII inhibited asymmetrical flagellar bending of intact and demembranated bull sperm (Ignotz and Suarez, 2005). There is evidence of additional Ca^{2+}-binding proteins in sperm flagella, such as calcium-binding tyrosine phosphorylation-regulated protein (CABYR) in mammals (Naaby-Hansen *et al.*, 2002) that could also play a role in modulating flagellar bending patterns.

Mathematical models of Ca^{2+} dynamics

Hyperactivation is known to be Ca^{2+} dependent and vital for fertilization, but how hyperactivation is triggered *in vivo* is still unknown. Experiments have provided insight into the signaling pathway, but there is no detailed understanding of how the channels, stores and clearance mechanisms are acting together to lead to hyperactivation. Along with experiments, mathematical models can be used to investigate non-linear interactions in the Ca^{2+} signaling pathway, and provide a systematic approach to examine the implications of hypothesized mechanisms of Ca^{2+} signaling in sperm.

Since Ca^{2+} is a universal signaling molecule, mathematical models of Ca^{2+} dynamics have been developed for many cell types including endocrine cells of the pituitary gland (Blum *et al.*, 2000), airway epithelial cells (Sneyd *et al.*, 1995), pancreatic and parotid acinar cells (Sneyd *et al.*, 2003), kidney epithelial cells (Roose *et al.*, 2006), vertebrate olfactory receptor neurons (Dougherty *et al.*, 2005), airway and pulmonary arteriole smooth muscle (Wang *et al.*, 2008) and the Xenopus oocyte (Atri *et al.*, 1993). Mathematical models that are based upon ordinary differential equations track the spatially averaged Ca^{2+} concentration in the sperm cell, and do not account for the location of channels and internal stores. Partial differential equation models are more detailed and track both the temporal and spatial evolution of Ca^{2+} in a cell or group of cells. The partial differential equation model presented in Olson *et al.* (2010) examines fluxes of Ca^{2+} due to channels and stores at the appropriate spatial location. In addition, spatial models may include the diffusion of ions along the length of the flagellum. Moreover, the diffusivity may also be spatially varying due to the microtubules, fibers, mitochondria, acrosome, nucleus and Jensen's ring. Olson *et al.* (2010) use a one-dimensional model, that represents the flagellum as a line, and assume a constant diffusion coefficient as a first approximation. Buffering of ions such as Ca^{2+} can play a large role in changing the free Ca^{2+}. Initial modeling efforts assume fast buffering, corresponding to effective fluxes and only account for a free Ca^{2+} concentration. It is noted that as models are extended from one-dimensional to higher dimensions, special considerations will need to be taken to model the flagellum as a tapering cylinder, and to accurately account for many of the structures within the flagellum.

In a mathematical model, the Ca^{2+} dynamics are determined by the specific extracellular signals (e.g. membrane depolarizations, neurotransmitters, shear stresses), key second messengers, the Ca^{2+} channels and clearance mechanisms, and the intracellular Ca^{2+} stores. Naturally, the components of the model are based upon experimental findings. However, even if some of the parameters (i.e. rate constants) are not known, overall dynamics can be measured for different ranges of parameter values, and the sensitivity of model results to changes in these parameters can be quantified. The model provides a platform to perform computational experiments that measure the effect of perturbing the system. These simulations could, for instance, correspond to pharmacologically inhibiting a channel or changing the extracellular Ca^{2+} concentration. The model can then be used to understand the relative importance of each mechanism, test hypotheses, and gain insight into the underlying physiology or cellular biology. Mathematical models can reveal interesting and unexpected relationships, suggesting experiments to be performed in the laboratory.

Ca^{2+} clearance model for mouse sperm

Wennemuth *et al.* (2003) performed a number of experiments on mouse sperm, including blocking Ca^{2+} channels and pumps, to understand the relative importance of specific Ca^{2+} clearance mechanisms of sperm. The fundamental questions were how do sperm maintain Ca^{2+} levels and remove excess Ca^{2+}? Through carefully designed experiments, they were able to understand the relative importance of each Ca^{2+} clearance mechanism after a depolarizing stimulus. The results of these experiments were used to set up a differential equation for the rate of change of Ca^{2+} concentration in the cytosol of the sperm. The Ca^{2+} fluxes accounted for were: (i) a constant leak flux into the cytosol, (ii) PMCA pumping Ca^{2+} out of the cytosol, (iii) MCU sequestering Ca^{2+}, (iv) a sodium–calcium (NCX) exchanger and (v) Ca^{2+} influx due to membrane depolarization. The system of ordinary differential equation was solved numerically to determine the spatially averaged Ca^{2+} concentration in the sperm cell. These concentrations were compared with experimental data

of spatially averaged Ca^{2+} concentrations determined using fluorescent Ca^{2+} indicators. Many qualitative features of the experimentally observed results were captured in the simulations. It was determined through experiments and simulations that the PMCA is the primary mechanism of Ca^{2+} clearance in mouse sperm after depolarization, with PMCA removing Ca^{2+} at a rate three times greater than the MCU and NCX. As discussed by Wennemuth *et al.* (2003), each of these fluxes is localized to a specific region, which is not taken into account in this model. The model also does not consider physiological and biochemical differences between activated and hyperactivated sperm.

CatSper-mediated Ca^{2+} dynamics model

In experiments by Xia *et al.* (2007), the relative intracellular Ca^{2+} concentration was recorded in mouse sperm after the application of a cell-permeant cAMP analog. The intracellular Ca^{2+} first started to increase in the principal piece, the location of the CatSper channels, and was followed by increases in Ca^{2+} along the length of the flagellum, with a sustained increase in the head region. After the initial increase in Ca^{2+}, Ca^{2+} clearance mechanisms brought the Ca^{2+} concentration back down to the basal, resting level. Xia *et al.* (2007) hypothesized that the cAMP analog facilitates the opening of the CatSper channels, causing Ca^{2+} influx in the principal piece through the CatSper channels, initiating a tail to head propagation of Ca^{2+} (Xia *et al.*, 2007). The main question they proposed is: can diffusion alone account for the sustained increase of Ca^{2+} in the head or is there some type of additional Ca^{2+} release that takes place due to the influx of Ca^{2+} from the CatSper channels?

We developed a one-dimensional reaction diffusion model to describe the CatSper-mediated Ca^{2+} dynamics associated with hyperactivation (Olson *et al.*, 2010), based on the experimental setup and results of Xia *et al.* (2007). The goal of this work was to introduce a mathematical model of Ca^{2+} dynamics in mammalian sperm relevant to hyperactivated motility. With this model, we examined how the spatial and temporal evolution of Ca^{2+} along the flagellar centerline depends upon diffusion, non-linear fluxes, and the presence of a Ca^{2+} store. The preliminary model assumed that the flagellar centerline was stationary and flat, and accounted for fluxes in the principal piece due to: (i) Ca^{2+} influx through CatSper channels, (ii) a constant leak flux and (iii) PMCA pumping Ca^{2+} out of the cytosol. Following Wennemuth *et al.* (2003), the PMCA was assumed to be the primary mode of Ca^{2+} clearance. Numerical simulations of this partial differential equation model demonstrated that diffusion alone could not account for a sustained increase in Ca^{2+} concentration in the head, as observed in the experiments by Xia *et al.* (2007).

In order to achieve better agreement with these experimental results, the model was extended to account for additional flux terms at the site of the RNE, an internal Ca^{2+} store in the neck of the sperm. The equations governing this system are as follows:

$$\frac{\partial C}{\partial t} = D_c \frac{\partial^2 C}{\partial s^2} + J_{RNE,cyt} - J_{RNE,uptake} - J_{PMCA} + J_{leak} + J_{Cat} \quad (1)$$

$$\frac{\partial I}{\partial t} = D_I \frac{\partial^2 I}{\partial s^2} + IP3_{prod} - IP3_{deg} \quad (2)$$

Here, C is the Ca^{2+} concentration, I is the IP_3 concentration, and s is the location along the flagellar centerline and t is time. The ions Ca^{2+} and IP_3 have effective diffusion coefficients D_C and D_I, respectively. In particular, the Ca^{2+} fluxes J_{PMCA}, J_{leak} and J_{Cat} accounted for in this model (and also the initial starting model) are due to the PMCA, leak and CatSper channels, respectively. Additional fluxes accounted for are due to a resequestration flux of Ca^{2+} back into the RNE $J_{RNE,uptake}$, and a flux out of the RNE into the cytosol $J_{RNE,cyt}$, which is due to Ca^{2+} release from the RNE, dependent on the local IP3 concentration, and a small leak flux. The extended model accounts for the local concentration of IP_3, which changes due to production $IP3_{prod}$ and degradation $IP3_{deg}$. The Ca^{2+} release from the RNE was dependent on the local IP_3 and Ca^{2+} concentration. When IP3-gated Ca^{2+} release from the RNE was accounted for, the results of the computational simulations agree with the qualitative trends of the experimental data. The model achieves a sustained increase of Ca^{2+} in the head, and exhibited a tail to head propagation of Ca^{2+}, as shown in Fig. 2 (Olson *et al.*, 2010). Through the use of a simple mathematical model, we were able to demonstrate that diffusion alone cannot account for the sustained increase of Ca^{2+} in the head. We hope that this mathematical model motivates the performance of further experiments to understand the role of Ca^{2+} release from the RNE, the role of IP3 and how its concentration evolves in time, as well as to determine kinetic rate parameters of channels and pumps relevant to Ca^{2+} dynamics.

Role of mathematical models in the future

In order for sperm to propel themselves forward, they use an undulatory flagellar motion, which is an emergent property of a complex system that couples the external fluid dynamics, passive elastic properties of the sperm structure, active force generation of the dynein arms and chemical signaling. In order to fully understand how the sperm are able to reach the oocyte and swim efficiently through the reproductive tract by modifying its waveform, integrative models that account for each of these aspects are necessary (Fauci and Dillon, 2006). Models that account for the fluid–structure interaction assume the fluid flow is governed by the Stokes equations or the Navier Stokes equations. Using these equations, the flagellum exerts forces on the surrounding fluid, and the equations account for the fluid density and viscosity. Recent models have captured elements of the full fluid–structure interaction (for example, Gueron and Levit-Gurevich, 1998; Dillon *et al.*, 2007; Fu *et al.*, 2007).

Mathematical models that couple the relevant biochemistry with mechanics and hydrodynamics will be of great use in the future to understand the impact of Ca^{2+} dynamics on sperm motility. We have been working toward this end by exploring a model that couples Ca^{2+} dynamics along the moving flagellum, viscous fluid mechanics, and the elastic properties of the flagellum. We couple our previous calcium model for CatSper-mediated Ca^{2+} dynamics (Olson *et al.*, 2010) to a time-dependent, preferred curvature that drives flagellar bending. This target wave amplitude corresponding

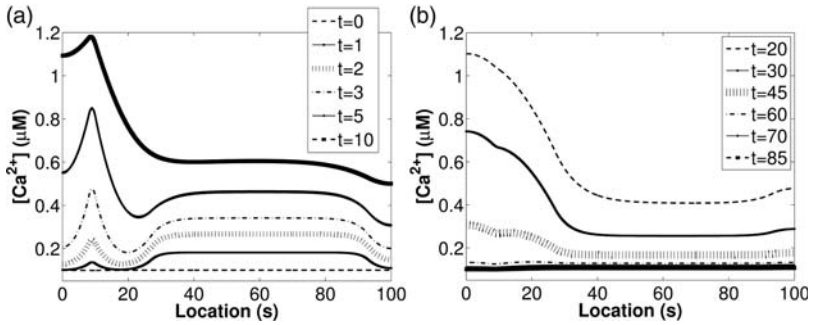

Figure 2 Simulations of the CatSper-mediated Ca^{2+} dynamics model described in Olson *et al.* (2010) and based on the experimental results of Xia *et al.* (2007). At $t = 0$, a cell-permeant cyclic nucleotide analog (8-Br-cAMP) was applied. The Ca^{2+} concentrations along the flagellum are shown, where $x = 0$ μm corresponds to the head and $x = 100$ μm corresponds to the endpiece of the flagellum. (**a**) Ca^{2+} first increases in the principal piece and then starts increasing in the neck, the location of the RNE. In this model, we account for IP_3-gated Ca^{2+} release from the RNE. Concentrations at later times are shown in (**b**). When the CatSper channels close and Ca^{2+} clearance mechanisms bring the Ca^{2+} concentration back to the resting level.

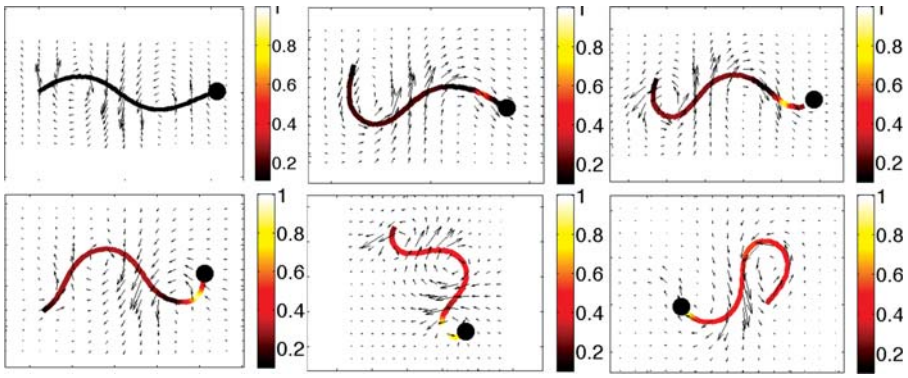

Figure 3 Simulations of a swimming sperm in a 3-dimensional viscous fluid where the CatSper-mediated Ca^{2+} dynamics are accounted for and are coupled to the preferred curvature. The solid black circle denotes the head side of the flagellum. Velocity vectors for the local fluid velocity are depicted in the plane of the beating flagellum and the calcium concentration along the length of the flagellum is shown. After application 8-Br-cAMP, the Ca^{2+} profiles (as in Fig. 2) are determined by the partial differential equations accounting for release of Ca^{2+} from the RNE. These Ca^{2+} concentrations are then used to define a preferred curvature for the flagellar waveform using a modified Hill function for the amplitude. From left to right, top row: $t = 0$, 1, 2 s and bottom row: $t = 4$, 6, 8 s. Note how the waveform is modified as the Ca^{2+} concentration increases.

to the preferred curvature is chosen to depend on the local Ca^{2+} concentration. In order to reflect the dependence of dynein force generation on Ca^{2+}, we used a modified Hill function to define the target amplitude $b(s, t)$,

$$b(s, t) = V_A \frac{\mathrm{Ca}(s, t)}{\mathrm{Ca}(s, t) + k_A} \tag{3}$$

Here, k_A is a coefficient for receptor activation, V_A is the maximum amplitude and $\mathrm{Ca}(s, t)$ is the Ca^{2+} concentration at time t and location along the flagellum s. In order to account for an asymmetry in the model, we designate a principal and reverse bend direction by monitoring the curvature along the length of the flagellum, and we set $k_A = k_{A,1}$ for positive curvature and $k_A = k_{A,2}$. Choosing $k_{A,1} \neq k_{A,2}$ assumes that different sides of the flagellum have different binding affinities for Ca^{2+} or a different number of binding sites.

In this model, the waveform of the flagellum is not pre-set, but is an emergent property of the coupled system. By including a slight asymmetry in the curvature model that reflects a hypothesized asymmetry in the axoneme's response to calcium, we observe the transition from activated motility to hyperactivated motility (Olson *et al.*, 2011). Figure 3 shows some snapshots of a model flagellum as it achieves a swimming pattern characteristic of hyperactivation. We view this model as a starting point to investigate the biochemistry and mechanics of sperm motility. Future modeling efforts will involve accounting for discrete representations of the dynein arms (for example Dillon *et al.*, 2007), whose activation kinetics will be governed by the evolving Ca^{2+} dynamics.

Authors' roles

S.D.O. wrote the initial draft of this invited review article; S.S.S. critically revised the biological portion of the draft; L.J.F. critically revised the mathematical portion. All three authors worked together on final revisions.

Funding

This work was supported by National Institutes of Health [1RO3HD062471-01] to SSS.

References

Arnoult C, Cardullo RA, Lemos JR, Florman HM. Activation of mouse T-type Ca^{2+} channels by adhesion to the egg zona pellucida. *Proc Natl Acad Sci USA* 1996;**93**:13004–13009.

Atri A, Amundson J, Clapham D, Sneyd J. A single-pool model for intracellular calcium oscillations and waves in the Xenopus laevis oocyte. *Biophys J* 1993;**65**:1727–1739.

Baldi E, Luconi M, Bonaccorsi L, Forti G. Nongenomic effects of progesterone on spermatozoa: mechanisms of signal transduction and clinical implications. *Front Biosci* 1998;**3**:1051–1059.

Bannai H, Yoshimura M, Takahashi K, Shingyoji C. Calcium regulation of microtubule sliding in reactivated sea urchin sperm flagella. *J Cell Sci* 2000;**113**:831–839.

Bedu-Addo K, Barratt CL, Kirkman-Brown JC, Publicover SJ. Patterns of $[Ca^{2+}](i)$ mobilization and cell response in human spermatozoa exposed to progesterone. *Dev Biol* 2007;**302**:324–332.

Bedu-Addo K, Costello S, Harper C, Machado-Oliveira G, Lefievre L, Ford C, Barratt C, Publicover S. Mobilisation of stored calcium in the neck region of human sperm—a mechanism for regulation of flagellar activity. *Int J Dev Biol* 2008;**52**:615–626.

Bendahmane M, Lynch C, Tulsiani DR. Calmodulin signals capacitation and triggers the agonist-induced acrosome reaction in mouse spermatozoa. *Arch Biochem Biophys* 2001;**390**:1–8.

Benoff S. Voltage dependent calcium channels in mammalian spermatozoa. *Front Biosci* 1998;**3**:1220–1240.

Blum JJ, Reed MC, Janovick JA, Conn PM. A mathematical model quantifying GnRH-induced LH secretion from gonadotropes. *Am J Physiol Endocrinol Metab* 2000;**278**:263–272.

Brokaw CJ. Calcium-induced asymmetrical beating of triton-demembranated sea urchin sperm flagella. *J Cell Bio* 1979;**82**:401–411.

Carlson AE, Westenbroek RE, Quill T, Ren D, Clapham DE, Hille B, Garbers DL, Babcock DF. CatSper1 required for evoked Ca^{2+} entry and control of flagellar function in sperm. *Proc Natl Acad Sci USA* 2003;**100**:14864–14868.

Carlson AE, Quill TA, Westenbroek RE, Schuh SM, Hille B, Babcock DF. Identical phenotypes of CatSper1 and CatSper2 null sperm. *J Biol Chem* 2005;**280**:32238–32244.

Carlson AE, Hille B, Babcock DF. External Ca^{2+} acts upstream of adenylyl cyclase SACY in the bicarbonate signaled activation of sperm motility. *Dev Biol* 2007;**312**:69–74.

Castellano LE, Trevino CL, Rodriguez D, Serrano CJ, Pacheco J, Tsutsumi V, Felix R, Darszon A. Transient receptor potential (TRPC) channels in human sperm: expression, cellular localization and involvement in the regulation of flagellar motility. *FEBS Lett* 2003; **541**:69–74.

Catterall WA. Structure and regulation of voltage-gated Ca^{2+} channels. *Annu Rev Cell Dev Biol* 2000;**16**:521–555.

Chang H, Suarez SS. Rethinking the relationship between hyperactivation and chemotaxis in mammalian sperm. *Biol Reprod* 2010;**83**:507–513.

Chang H, Suarez SS. Two distinct Ca2+ signaling pathways modulate sperm flagellar beating patterns. *Biol Reprod* 2011. [Epub ahead of print] PMID 2138934.

Chen Y, Cann MJ, Litvin TN, Iourgenko V, Sinclair ML, Levin LR, Buck J. Soluble adenylyl cyclase as an evolutionarily conserved bicarbonate sensor. *Science* 2000;**289**:625–628.

Costello S, Michelangeli F, Nash K, Lefievre L, Morris J, Machado-Oliveira G, Barratt C, Kirkman-Brown J, Publicover S. Ca2+-stores in sperm: their identities and functions. *Reproduction* 2009;**138**:425–437.

DeMott RP, Suarez SS. Hyperactivated sperm progress in the mouse oviduct. *Biol Reprod* 1992;**46**:779–785.

Dillon R, Fauci L, Omoto C, Yang X. Fluid dynamic models of flagellar and ciliary beating. *Ann NY Acad Sci* 2007;**1101**:494–505.

Dougherty DP, Wright GA, Yew AC. Computational model of the cAMP-mediated sensory response and calcium-dependent adaptation in vertebrate olfactory receptor neurons. *Proc Natl Acad Sci USA* 2005; **102**:10415–10420.

Eisenbach E. A hitchhikers guide through advances and conceptual changes in chemotaxis. *J Cell Physiol* 2007;**213**:574–580.

Eltit JM, Feng W, Lopez JR, Padilla IT, Pessah IN, Molinski TF, Fruen BR, Allen PD, Perez CF. Ablation of skeletal muscle triadin impairs FKBP12/RyR1 channel interactions essential for maintaining resting cytoplasmic Ca2+. *J Biol Chem* 2010;**285**:38453–38462.

Ertel EA, Campbell KP, Harpold MM, Hofmann F, Mori Y, Perez-Reyes E, Schwartz A, Snutch TP, Tanabe T, Birnbaumer L *et al*. Nomenclature of voltage-gated calcium channels. *Neuron* 2000;**25**:533–535.

Fauci LJ, Dillon R. Biofluidmechanics of reproduction. *Annu Rev Fluid Mech* 2006;**38**:371–394.

Felix R. Molecular physiology and pathology of Ca^{2+}-conducting channels in the plasma membrane of mammalian sperm. *Reproduction* 2005; **129**:251–262.

Fu H, Powers TR, Wolgemuth CW. Theory of swimming filaments in viscoelastic media. *Phys Rev Lett* 2007;**99**:258101–05.

Gueron S, Levit-Gurevich K. Computation of the internal forces in cilia: application to ciliary motion, the effects of viscosity, and cilia interactions. *Biophys J* 1998;**74**:1658–1676.

Gunter TE, Buntinas G, Sparagna G, Eliseev R, Gunter K. Mitochondrial calcium transport: mechanisms and functions. *Cell Calcium* 2000; **28**:285–296.

Gwathmey TM, Ignotz GG, Suarez SS. PDC-109 (BSP-A1/A2) promotes bull sperm binding to oviductal epithelium in vitro and may be involved in forming the oviductal sperm reservoir. *Biol Reprod* 2003; **69**:809–815.

Gwathmey TM, Ignotz GG, Mueller JM, Manjunath P, Suarez SS. Bovine seminal plasma proteins PDC-109, BSP-A3, and BSP-30-kDa share functional roles in storing sperm in the oviduct. *Biol Reprod* 2006; **75**:501–507.

Harper CV, Barratt CLR, Publicover SJ. Stimulation of human spermatozoa with progesterone gradients to simulate approach to the oocyte. *J Biol Chem* 2004;**279**:46315–46325.

Harper C, Wootton L, Michelangeli F, Lefievre L, Barratt C, Publicover S. Secretory pathway Ca^{2+}-ATPase (SPCA1) Ca^{2+} pumps, not SERCAs, regulate complex $[Ca^{2+}]_i$ signals in human spermatozoa. *J Cell Sci* 2005;**118**:1673–1685.

Herrick SB, Schweissinger DL, Kim SW, Bryan KR, Mann S, Cardullo RA. The acrosomal vesicle of mouse sperm is a calcium store. *J Cell Physiol* 2005;**202**:663–C671.

Ho HC, Suarez SS. Hyperactivation of mammalian spermatozoa: function and regulation. *Reproduction* 2001a;**122**:519–526.

Ho HC, Suarez SS. An inositol 1,4,5-trisphosphate receptor-gated intracellular Ca^{2+} store is involved in regulating sperm hyperactivated motility. *Biol Reprod* 2001b;**65**:1606–1615.

Ho HC, Suarez SS. Characterization of the intracellular calcium store at the base of the sperm flagellum that regulates hyperactivated motility. *Biol Reprod* 2003;**68**:1590–1596.

Ho HC, Granish KA, Suarez SS. Hyperactivated motility of bull sperm is triggered at the axoneme by Ca^{2+} and not cAMP. *Dev Biol* 2002; **250**:208–217.

Ho K, Wolff CA, Suarez SS. CatSper-null mutant spermatozoa are unable to ascend beyond the oviductal reservoir. *Reprod Fertil Dev* 2009; **21**:345–350.

Ignotz GG, Suarez SS. Calcium/calmodulin and calmodulin kinase II stimulate hyperactivation in demembranated bovine sperm. *Biol Reprod* 2005;**73**:519–526.

Ignotz GG, Cho MY, Suarez SS. Annexins are candidate oviductal receptors for bovine sperm surface proteins and thus may serve to hold bovine sperm in the oviductal reservoir. *Biol Reprod* 2007; **77**:906–913.

Ishijima S, Mohri H, Overstreet JW, Yudin AI. Hyperactivation of monkey spermatozoa is triggered by Ca^{2+} and completed by cAMP. *Mol Reprod Dev* 2006;**73**:1129–1139.

Jimenez-Gonzalez C, Michelangeli F, Harper CV, Barratt CL, Publicover SJ. Calcium signalling in human spermatozoa: a specialized 'toolkit' of channels, transporters, and stores. *Hum Reprod Update* 2006; **12**:253–267.

Jin J, Jin N, Zheng H, Ro S, Tafolla D, Sanders KM, Yan W. CatSper3 and CatSper4 are essential for sperm hyperactivated motility and male fertility in the mouse. *Biol Reprod* 2007;**77**:37–44.

Kanous KS, Casey C, Lindemann CB. Inhibition of microtubule sliding by Ni^{2+} and Cd^{2+}: evidence for a differential response of certain microtubule pairs within the bovine sperm axoneme. *Cell Motil Cytoskeleton* 1993;**26**:66–76.

Katz DF, Yanagimachi R. Movement characteristics of hamster spermatozoa within the oviduct. *Biol Reprod* 1980;**22**:759–764.

Kervancioglu ME, Djahanbakhch O, Aitken RJ. Epithelial cell coculture and the induction of sperm capacitation. *Fertil Steril* 1994;**61**:1103–1108.

Kirichok Y, Navarro B, Clapham DE. Whole cell patch clamp measurements of spermatozoa reveal an alkaline-activated Ca^{2+} channel. *Nature* 2006;**439**:737–740.

Krasznai Z, Krasznai ZT, Morisawa M, Bazsane ZK, Hernadi Z, Fazekas Z, Tron L, Goda K, Marian T. Role of the Na^{+}/Ca^{2+} exchanger in calcium homeostasis and human sperm motility regulation. *Cell Motil Cytoskeleton* 2006;**63**:66–76.

Lawson C, Dorval V, Goupil S, Leclerc P. Identification and localisation of SERCA 2 isoforms in mammalian sperm. *Mol Hum Reprod* 2007; **13**:307–316.

Lindemann CB, Goltz JS. Calcium regulation of flagellar curvature and swimming pattern in triton X-100 extracted rat sperm. *Cell Motil Cytoskeleton* 1988;**10**:420–431.

Lindemann CB, Kanous KS. Geometric clutch hypothesis of axonemal function: key issues and testable predictions. *Cell Motil Cytoskeleton* 1995;**31**:1–8.

Lindemann CB, Lesich KA. Flagellar and ciliary beating: the proven and the possible. *J Cell Sci* 2010;**123**:519–528.

Lindemann CB, Walker JM, Kanous KS. Ni^{2+} inhibition induces asymmetry in axonemal functioning and bend initiation of bull sperm. *Cell Motil Cytoskeleton* 1995;**30**:8–16.

Liu J, Xia J, Cho KH, Clapham DE, Ren D. CatSperbeta, a novel transmembrane protein in the CatSper channel complex. *J Biol Chem* 2007;**282**:18945–18952.

Lloyd RE, Badia E, Fazeli A, Watson PF, Holt WV. Temporal dynamics of ram sperm binding and survival during 48-h coculture with oviducal epithelial cells. *Reprod Fertil Dev* 2008;**20**:835–845.

Lobley A, Pierron V, Reynolds L, Allen L, Michalovich D. Identification of human and mouse CatSper3 and CatSper4 genes: characterisation of a common interaction domain and evidence for expression in testis. *Reprod Biol Endocrinol* 2003;**1**:53–67.

Marin-Briggiler CI, Jha KN, Chertihin O, Buffone MG, Herr JC, Vazquez-Levin MH, Visconti PE. Evidence of the presence of calcium/calmodulin-dependent protein kinase IV in human sperm and its involvement in motility regulation. *J Cell Sci* 2005;**118**:2013–2022.

Marquez B, Suarez SS. Different signaling pathways in bovine sperm regulate capacitation and hyperactivation. *Biol Reprod* 2004; **70**:1626–1633.

Marquez B, Suarez SS. Bovine sperm hyperactivation is promoted by alkaline-stimulated Ca^{2+} influx. *Biol Reprod* 2007;**76**:660–665.

Marquez B, Ignotz G, Suarez SS. Contributions of extracellular and intracellular Ca^{2+} regulation of sperm motility: release of intracellular stores can hyperactivate CatSper1 and CatSper2 null sperm. *Dev Biol* 2007;**303**:214–221.

Mattner PE. The distribution of spermatozoa and leucocytes in the female genital tract in goats and cattle. *J Reprod Fertil* 1968;**17**:253–261.

Means AR, Tash JS, Chafouleas JG. Physiological implications of the presence, distribution, and regulation of calmodulin in eukaryotic cells. *Physiol Rev* 1982;**62**:1–39.

Meizel S, Turner KO. Initiation of the human sperm acrosome reaction by thapsigargin. *J Exp Zool* 1993;**267**:350–355.

Mullins KJ, Saacke RG. Study of the functional anatomy of bovine cervical mucosa with special reference to mucus secretion and sperm transport. *Anat Rec* 1989;**225**:106–117.

Naaby-Hansen S, Mandal A, Wolkowicz MJ, Sen B, Westbrook VA, Shetty J, Coonrod SA, Klotz KL, Kim YH, Bush LA *et al.* CABYR, a novel calcium-binding tyrosine phosphorylation-regulated fibrous sheath protein involved in capacitation. *Dev Biol* 2002;**242**:236–254.

Navarro B, Kirkchok Y, Clapham DE. KSper, a pH-sensitive K^{+} current that controls sperm membrane potential. *Proc Natl Acad Sci USA* 2007;**104**:7688–7692.

Nicholls DJ, Chalmers S. The integration of mitochondrial calcium transport and storage. *J Bioenerg Biomembr* 2004;**36**:1573–6881.

Okunade GW, Miller ML, Pyne GJ, Sutliff RL, O'Connor KT, Neumann JC, Andringa A, Miller DA, Prasad V, Doetschman T *et al.* Targeted ablation of plasma membrane Ca^{2+}-ATPase (PMCA) 1 and 4 indicates a major housekeeping function for PMCA1 and a critical role in hyperactivated sperm motility and male fertility for PMCA4. *J Biol Chem* 2004; **279**:33742–33750.

Olson SD, Suarez SS, Fauci LJ. A model of CatSper channel mediated calcium dynamics in mammalian spermatozoa. *Bull Math Biol* 2010; **72**:1925–1946.

Olson SD, Suarez SS, Fauci LJ. Coupling biochemistry and hydrodynamics captures hyperactivated sperm motility in a simple flagellar model. *J Theor Biol* 2011; in press.

Osman RA, Andria ML, Jones AD, Meizel S. Steroid induced exocytosis: the human sperm acrosome reaction. *Biochem Biophys Res Commun* 1989;**160**:828–833.

O'Toole CM, Arnoult C, Darszon A, Steinhardt RA, Florman HM. Ca2+ entry through store-operated channels in mouse sperm is initiated by egg ZP3 and drives the acrosome reaction. *Mol Biol Cell* 2000; **11**:1571–1584.

Parpura V, Haydon PG. Physiological astrocytic calcium levels stimulate glutamate release to modulate adjacent neurons. *Proc Natl Acad Sci USA* 2000;**97**:8629–8634.

Pollard JW, Plante C, King WA, Hansen PJ, Betteridge KJ, Suarez SS. Fertilizing capacity of bovine sperm may be maintained by binding of oviductal epithelial cells. *Biol Reprod* 1991;**44**:102–107.

Qi H, Moran MM, Navarro B, Chong JA, Krapivinsky G, Krapivinsky L, Kirichok Y, Ramsey IS, Quill TA, Clapham DE. All four CatSper ion channel proteins are required for male fertility and sperm cell hyperactivated motility. *Proc Natl Acad Sci USA* 2007;**104**:1219–1223.

Quill TA, Ren D, Clapham DE, Garbers DL. A voltage-gated ion channel expressed specifically in spermatozoa. *Proc Natl Acad Sci USA* 2001; **98**:12527–12531.

Quill T, Sugden SA, Rossi KL, Doolittle LK, Hammer RE, Garbers DL. Hyperactivated sperm motility driven by CatSper2 is required for fertilization. *Proc Natl Acad Sci USA* 2003;**100**:14869–14874.

Ren D, Navarro B, Perez G, Jackson AC, Hsu S, Shi Q, Tilly JL, DE Clapham DE. A sperm ion channel required for sperm motility and male fertility. *Nature* 2001;**413**:603–609.

Roose T, SJ Chapman SJ, PK Maini PK. A mathematical model for simultaneous spatio-temporal dynamics of calcium and inositol 1,4,5-trisphosphate in Madin-Darby canine kidney epithelial cells. *Bull Math Biol* 2006;**68**:2027–2051.

Sakata Y, Saegusa H, Zong S, Osanai M, Murakoshi T, Shimizu Y, Noda T, Aso T, Tanabe T. $Ca_v2.3$ (α1E) Ca^{2+} channel participates in the control of sperm function. *FEBS Lett* 2002;**516**:229–233.

San Agustin JT, Witman GB. Role of cAMP in the reactivation of demembranated ram spermatozoa. *Cell Motil Cytoskeleton* 1994; **27**:206–218.

Schlingmann K, Michaut MA, McElwee JL, Wolff CA, Travis AJ, Turner RM. Calmodulin and CaMKII in the sperm principal piece: evidence for a motility-related calcium/calmodulin pathway. *J Androl* 2007; **28**:706–716.

Schuh K, Cartwright EJ, Jankevics E, Bundschu K, Liebermann J, Williams JC, Armesilla AL, Emerson M, Oceandy D, Knobeloch KP *et al.* Plasma membrane Ca^{2+} ATPase 4 is required for sperm motility and male fertility. *J Biol Chem* 2004;**279**:28220–28226.

Shalgi R, Smith TT, Yanagimachi R. A quantitative comparison of the passage of capacitated and uncapacitated hamster spermatozoa through the uterotubal junction. *Biol Reprod* 1992;**46**:419–424.

Smith TT, Koyanagi F, Yanagimachi R. Quantitative comparison of the passage of homologous and heterologous spermatozoa through the uterotubal junction of the golden hamster. *Gamete Res* 1988; **19**:227–234.

Sneyd J, Wetton BTR, Charles AC, Sanderson MJ. Intercellular calcium waves mediated by diffusion of inositol trisphosphate - a two-dimensional model. *Am J Physiol* 1995;**268**:C1537–C1545.

Sneyd J, Tsaneva-Atanasova K, Bruce JI, Straub SV, Giovannucci DR, Yule DI. A model of calcium waves in pancreatic and parotid acinar cells. *Biophys J* 2003;**85**:1392–1405.

Spehr M, Gisselmann G, Poplawski A, Riffell JA, Wetzel CH, Zimmer RK, Hatt H. Identification of a testicular odorant receptor mediating human sperm chemotaxis. *Science* 2003;**299**:2054–2058.

Spehr M, Schwane K, Riffell JA, Barbour J, Zimmer RK, Neuhaus EM, Hatt H. Particulate adenylate cyclase plays a key role in human sperm olfactory receptor-mediated chemotaxis. *J Biol Chem* 2004; **279**:40194–40203.

Stauss CR, Votta TJ, Suarez SS. Sperm motility hyperactivation facilitates penetration of the hamster zona pellucida. *Biol Reprod* 1995; **53**:1280–1285.

Suarez SS. Control of hyperactivation in sperm. *Hum Reprod Update* 2008; **14**:647–657.

Suarez SS. How do sperm get to the egg? Bioengineering expertise needed! *Exp Mech* 2010;**50**:1267–1274.

Suarez SS, Dai X. Hyperactivation enhances mouse sperm capacity for penetrating viscoelastic media. *Biol Reprod* 1992;**46**:686–691.

Suarez SS, Osman RA. Initiation of hyperactivated flagellar bending in mouse sperm within the female reproductive tract. *Biol Reprod* 1987; **36**:1191–1198.

Suarez SS, Pacey AA. Sperm transport in the female reproductive tract. *Hum Reprod Update* 2006;**12**:23–37.

Suarez SS, Vincenti L, Ceglia MW. Hyperactivated motility induced in a mouse sperm by calcium ionophore A23187 is reversible. *J Exp Zool* 1987;**244**:331–336.

Suarez SS, Katz DF, Owen DH, Andrew JB, Powell RL. Evidence for the function of hyperactivated motility in sperm. *Biol Reprod* 1991; **44**:375–381.

Suarez SS, Dai XB, DeMott RP, Redfern K, Mirando MA. Movement characteristics of boar sperm obtained from the oviduct or hyperactivated in vitro. *J Androl* 1992;**13**:75–80.

Suarez SS, Varosi SM, Dai X. Intracellular calcium increases with hyperactivation in intact, moving hamster sperm and oscillates with the flagellar beat cycle. *Proc Natl Acad Sci USA* 1993;**90**: 4660–4664.

Tash JS, Means AR. Regulation of protein phosphorylation and motility of sperm by cyclic adenosine monophosphate and calcium. *Biol Reprod* 1982;**26**:745–763.

Tash JS, Means AR. Cyclic adenosine 3′, 5′ monophosphate, calcium, and protein phosphorylation in flagellar motility. *Biol Reprod* 1983; **28**:75–104.

Teves ME, Barbano F, Guidobaldi HA, Sanchez R, Miska W, Giojalas LC. Progesterone at the picomolar range is a chemoattractant for mammalian spermatozoa. *Fertil Steril* 2006;**86**:745–749.

Thastrup O, Cullen PJ, Drobak BK, Hanley MR, Dawson A. Thapsigargin, a tumor promoter, discharges intracellular Ca2+ stores by specific inhibition of the endoplasmic reticulum Ca2+-ATPase. *Proc Natl Acad Sci USA* 1990;**87**:2466–2470.

Trevino CL, Serrano CJ, Beltran C, Felix R, Darszon A. Identification of mouse TRP homologs and lipid rafts from spermatogenic cells and sperm. *FEBS Lett* 2001;**509**:119–125.

Trevino CL, Felix R, Castellano LE, Gutierrez C, Rodriguez D, Pacheco J, Lopez-Gonzalez I, Gomora JC, Tsutsumi V, Hernandez-Cruz A *et al.* Expression and differential cell distribution of low-threshold Ca^{2+} channels in mammalian male germ cells and sperm. *FEBS Lett* 2004; **563**:87–92.

Turner RM. Tales from the tail: what do we really know about sperm motility? *J Androl* 2003;**24**:790–803.

Visconti PE. Understanding the molecular basis of sperm capacitation through kinase design. *Proc Natl Acad Sci USA* 2009;**106**:667–668.

Walensky LD, Snyder SH. Inositol 1,4,5-trisphosphate receptors selectively localized to the acrosomes of mammalian sperm. *J Cell Biol* 1995;**130**:857–869.

Wang I, Politi A, Tania N, Bai Y, Sanderson MJ, Sneyd J. A mathematical model of airway and pulmonary arteriole smooth muscle. *Biophys J* 2008;**94**:2053–2064.

Wang H, Liu J, Cho KH, Ren D. A novel, single, transmembrane CATSPERG is associated with CATSPER1 channel protein. *Biol Reprod* 2009;**81**:539–544.

Weinmann S, Ores-Carton C, Rainteau D, Puszkin S. Immunoelectron microscopic localization of calmodulin and phospholipase A2 in spermatozoa. I. *J Histochem Cytochem* 1986;**34**:1171–1179.

Wennemuth G, Westenbroek RW, Xu T, Hille B, Babcock DF. Cav 2.2 and Cav 2.3 (N- and R-type) Ca^{2+} channels in depolarization-evoked entry of Ca^{2+} into mouse sperm. *J Biol Chem* 2000; **275**:21210–21217.

Wennemuth G, Babcock DF, Hille B. Calcium clearance mechanisms of mouse sperm. *J Gen Physiol* 2003;**122**:115–128.

Westenbroek RE, Babcock DF. Discrete regional distributions suggest diverse functional roles of calcium channel α1 subunits in sperm. *Dev Biol* 1999;**207**:457–469.

Wiesner B, Weiner J, Middendorff R, Hagen V, Kaupp UB, Weyand I. Cyclic nucleotide-gated channels on the flagellum control Ca^{2+} entry into sperm. *J Cell Biol* 1998;**142**:473–484.

Wuytack F, Raeymaekers L, Missiaen L. Molecular physiology of the SERCA and SPCA pumps. *Cell Calcium* 2002;**32**:279–305.

Xia J, Reigada D, Mitchell CH, Ren D. CATSPER channel-mediated Ca^{2+} entry into mouse sperm triggers a tail-to-head propagation. *Biol Reprod* 2007;**77**:551–559.

Yanagimachi R. Mammalian fertilization. In: Knobil E, Neil JD (eds). *The Physiology of Reproduction*, 2nd edn. New York, NY: Raven Press, 1994, 189–317.

Yanamaguchi R, Muro Y, Isotani A, Tokuhiro K, Takumi K, Adham I, Ikawa M, Okabe M. Disruption of ADAM3 impairs the migration of sperm into oviduct in mouse. *Biol Reprod* 2009; **81**:142–146.